This is the accept manuscript of the following article that appeared in final form in Theoretical and Applied Fracture Mechanics 87: 99-109 (2017), which has been published in final form at https://doi.org/10.1016/j.tafmec.2016.11.001.

Equivalent energy release rate and crack stability in the End Notched Flexure with inserted roller mixed mode I/II test

A. Boyano*[a], J. De Gracia[a], A. Arrese[b], F. Mujika[b]

[a,b] Materials + Technologies Group, Department of Mechanical Engineering
[a] Faculty of Engineering of Vitoria-Gasteiz, University of the Basque Country (UPV/EHU)
Nieves Cano, 12, 01006 Vitoria-Gasteiz, Spain
*e-mail: ana.boyano@ehu.eus // Tel: +34 945 013933
[b] Faculty of Engineering of Gipuzkoa - University of the Basque Country (UPV/EHU)
Plaza de Europa, 1, 20018 San Sebastian, Spain

Abstract

The crack propagation performance of the End Notched Flexure with inserted roller test is analyzed. An equivalent energy release rate is proposed taking into account the interaction of the modes I and II, based on the linear failure criterion. Experimental results obtained with specimens of F593/T300 carbon/epoxy unidirectional composite show a good agreement with the proposed approach. The stability condition is theoretically developed based on the derivative of the equivalent energy release rate, under fixed load condition and fixed displacement condition. Experimental tests have been carried out to assess the proposed equivalent energy release rate and to evaluate the crack stability condition. An analysis of the influence of compliance measurement on the crack length and on the equivalent energy release rate is included. Based on the results obtained, test conditions with initial mode ratios between 65% and 75% are recommended.

Keywords: Composites; Delamination; Mixed-mode; Energy Release Rate; Crack Stability.

1 INTRODUCTION

One of the main objectives in fracture mechanics is to measure the fracture toughness of materials. It is supposed that a stable crack growth is required for reliable energy release rate curves determination.

Different type of test configurations have been used to investigate the mixed-mode I/II fracture of different materials, such as composite laminates [1-3], wood [4-6], or adhesively bonded joints [7-11]. However, the stability condition of the mixed-mode test is not defined in the standard. The only mention done is that in the high mode II regime, the delamination growth is often unstable, precluding propagation toughness values from being determined. It is also stated that the use of longer initial delaminations increases the tendency for stable delamination growth [12]. With respect to pure modes I and II, the Double Cantilever Beam test (DCB) is considered always stable [13], and the End Notched Flexure test (ENF) is stable if a/L>0.7 [14,15].

Phillips and Wells [16], studied the stability of transverse cracks in composites. They assumed as stability limit the derivative of stress with respect to the crack length obtaining a critical value. If the initial crack is less than the critical one, the crack propagates unstably at a stress value determined by the initial fracture energy and it grows spontaneously under decreasing load. On the contrary, cracks which are initially larger than the critical size are stable and only grow if the load increases.

Allix and Corigliano [17] dealt with the problem of simulating the mixed-mode I/II crack propagation. They compared the analytical results from the Linear Elastic Fracture Mechanics (LEFM) hypotheses and numerical results concerning crack stability of the Asymmetric End Loaded Split (AELS) specimen. The analytical results stated that under load control it was always unstable and under displacement control the stability condition was a/L>0.42. By means of the nonlinear numerical model proposed, the limit for stable crack propagation under displacement control was a/L =0.435 which is very close to the analytical result.

Szekrenyes [18], verified the traditional compliance based criterion, based on the derivative of the energy release rate (ERR) by experimental observations. He used transparent material to visually measure crack length and crack propagation. The transition from stability to instability was defined as the point just before a crack jump. He found that the stability of the system depends on the derivative of the critical displacement defined as the displacement of the load application point at crack initiation. The relationship between the critical displacement and the crack length was determined by experiments in many specimens of different initial crack lengths, for different test methods. The critical value of crack length was determined by differentiation after curve fitting of experimental data. He deduced that the point of instability was always where the critical displacement reached its minimum value.

In the present work the crack propagation performance is analyzed in a mixed mode I/II End Notched Flexure specimen with inserted roller (ENFR), recently proposed [19,20]. Taking into account the interaction between the two modes, an equivalent energy release (ERR) concept has been developed and the stability condition has been determined by means of the derivative of that equivalent energy release rate. An error analysis has been carried out in order to determine the influence of compliance measurement on the crack length and on the equivalent ERR. Analyzing the experimental data during the propagation, the proposed equivalent ERR has been assessed and the crack stability has been evaluated. Optimum test conditions for tests performed under displacement control have been proposed.

NOMENCLATURE

$a, \Delta a$	crack length and crack increment, respectively
c_i	distances from the support to the position of the roller
$b, 2h$	width and thickness of the specimen, respectively
C_{spec}, C_s, C_{exp},	compliance of the specimen, of the system and experimental compliance, respectively
k_S	stiffness of the system
δ_0, P_0	initial displacement and initial load, respectively
δ	displacement of the middle point of the specimen
$\delta_{spec,}$ δ_{exp}	calculated and experimental displacement of the middle point of the specimen, respectively
E_f	flexural modulus
$G_{LT,}$ $G_{LT'}$	in-plane shear modulus and out of plane shear modulus, respectively
E_{11}, $E_{22,}$ G_{12}	longitudinal elastic modulus, transversal elastic modulus and shear elastic modulus respectively
G_I,G_{II} , G	energy release rates for mode I, mode II, and total, respectively
G_{Ic},G_{IIc} , G_c	critical energy release rate for mode I, mode II, and total, respectively
$G_{eq,}$$G_{eqc}$	equivalent energy release rate and critical equivalent energy release rate, respectively
$K_{Ca,}$ K_{aG}	error coefficients that correspond to the influence of the measurement of compliance on the crack length, and the influence of the determination of crack length on equivalent energy release rate, respectively.
L	half span of the test
P	applied Load
Y	force exerted by the roller
R	roller radius
W, U, U^*	work done by external forces, strain energy, and complementary strain energy, respectively

2 ANALYTICAL BACKGROUND

2.1 Compliance of ENFR test

The End Notched Flexure with inserted Roller (ENFR) test configuration has been proposed [19] and experimentally assesed [20] recently. In order to get mixed mode, a roller is introduced between the two surfaces of the crack and the specimen is tested in ENF configuration. The mode II is provided by the external load and the mode I is obtained by the opening of the crack due to the insertion of the roller as shown in Fig. 1. The roller can be located at the outer side or at the inner side of the support.

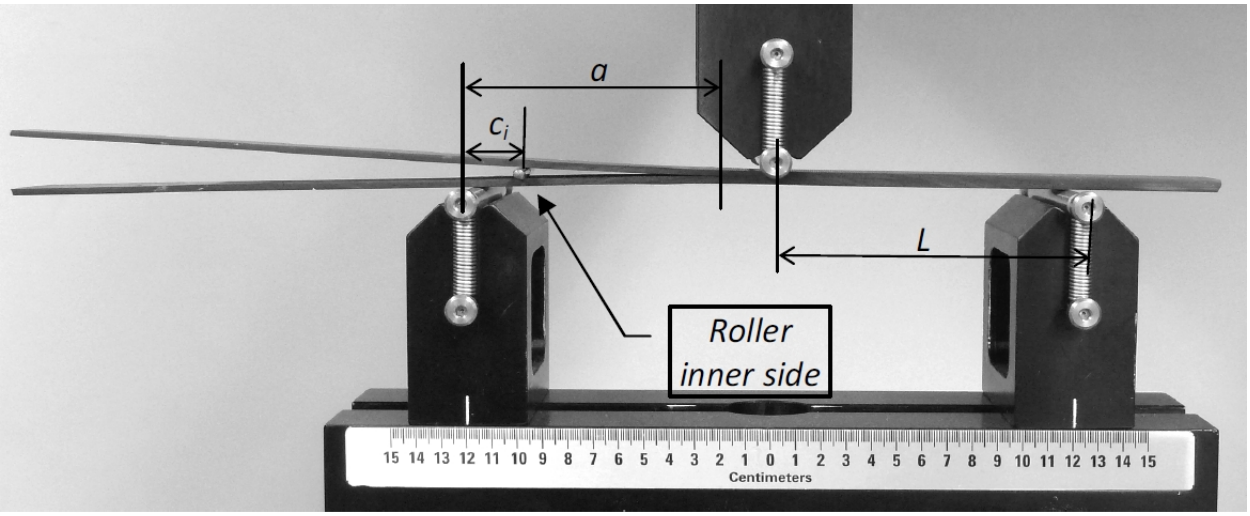

Fig. 1 ENFR Test configuration with the roller located at the inner side

Being *Y* the force exerted by the roller and being it the force that generates the displacement, taking into account only bending effects, when the roller is located at the inner side of the support, the *Y* force is [19]:

$$Y = \frac{R}{4}\frac{E_f b h^3}{(a-c)^3} + \frac{P(2a+c)}{8(a-c)} \tag{1}$$

Where *R* is the radius of the roller; *c* is the distance from the support where it is located; *a* is the crack length; *P* is the applied load; E_f the flexural modulus; *b* the width of the specimen; and *2h* the total thickness of the specimen.

The displacement of the load application point taking into account only bending effects is [19]:

$$\delta = \frac{P}{8E_f b h^3}(3a^3 + 2L^3 + c^3 + 3ac^2) - \frac{R}{4}\frac{(2a+c)}{(a-c)} \tag{2}$$

According to Eq.(2), due to the roller introduced between the specimen arms, there is an initial negative displacement without external load application. Furthermore, when the displacement is null, there is a positive load. The initial conditions can be calculated replacing P=0 and δ=0 in Eq.(2) and lead to [19]:

$$\delta_0 = -\frac{R}{4}\frac{(2a+c)}{(a-c)}$$
$$P_0 = \frac{2RE_f bh^3(2a+c)}{(a-c)(3a^3+c^3+2L^3+3ac^2)} \quad (3)$$

The theoretical load-displacement curve before crack propagation occurs is depicted in Fig. 2.

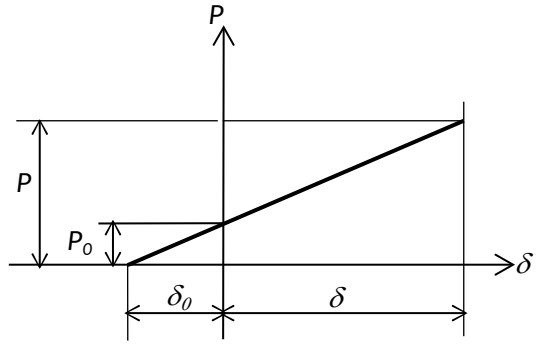

Fig. 2 Load-displacement curve for ENFR test before crack propagation

According to Fig. 2 the compliance of the ENFR test is [19]:

$$C = \frac{\delta}{P-P_0} = \frac{\delta_0}{P_0} = \frac{3a^3+2L^3+c^3+3ac^2}{8E_f bh^3} \quad (4)$$

2.2 Energy release rate in the ENFR test

According to Griffith [21] and Irwin [22], the energy balance in a small crack advance can be expressed as:

$$dW = dU + Gbda \quad (5)$$

Where dW is the work done by external forces; dU is the change in strain energy; G is the energy needed for the crack advance per unit area; b is the width of the crack; and da is the differential crack advance. The differential work done by the external forces F_i in their respective displacements δ_i, assuming the repeated index convention is $dW = F_i d\delta_i$. The complementary strain energy U* is defined as:

$$U^* = F_i\delta_i - U \quad (6)$$

Differentiating Eq.(6), and replacing in the energy balance equation of Eq.(5) it results:

$$dU^* = \delta_i dF_i + Gbda \quad (7)$$

In spite of the crack advance is an irreversible process, it is assumed that an elemental variation the complementary strain energy is an exact differential. Since the state variables are F_i and a, thus:

$$dU^* = \frac{\partial U^*}{\partial F_i} dF_i + \frac{\partial U^*}{\partial a} da \tag{8}$$

Identifying the first terms in Eq.(7) and Eq.(8) it results the theorem of Engesser-Castigliano. Identifying the second summands it results:

$$G = \frac{1}{b}\left(\frac{\partial U^*}{\partial a}\right)_{F_i cte} \tag{9}$$

In the ENFR test the work is done by two forces, *Y* and *P*. The work carried out by *Y* is related to the finite displacement imposed by the roller, and the work carried out by *P* is related to the application of the load. According to Eq.(9) the complementary strain energy must be used for determining *G* if forces are used as state variables.

When the roller is positioned at the inner side of the crack tip, taking into account only bending effects, the energy release due to each fracture mode can be expressed as follows [19]:

$$\begin{aligned} G_I &= \frac{3R^2 E_f h^3}{4(a-c)^4} + \frac{3PRc}{4b(a-c)^2} + \frac{3P^2 c^2}{16 E_f b^2 h^3} \\ G_{II} &= \frac{9P^2 a^2}{16 E_f b^2 h^3} \end{aligned} \tag{10}$$

The values of G_I and G_{II} of Eq. (10) agree with those obtained by William´s partition method [23]. In the case that c=0 and taking into account only bending effects, they agree with those obtained by Szekrenyes [24] for this test configuration.

In many cases *G* is determined based on the compliance, using the Irwin-Kies approach [25]. In the present case, the calculation of *G* based on the derivative of the compliance is:

$$G = \frac{P^2}{2b}\frac{dC}{da} = \frac{9P^2 a^2}{16 E_f b^2 h^3} + \frac{3P^2 c^2}{16 E_f b^2 h^3} \tag{11}$$

In Eq. (11) two summands corresponding mode I of Eq. (10) are not included. Then, in the present case the approach based on the compliance is not valid. It can be concluded that it is also valid in cases where the external work is carried out by a unique force.

3 EQUIVALENT ENERGY RELEASE RATE

Crack propagation only occurs if the energy available for a crack extension, G, is enough to provide all the energy that is required for crack growth [26]. The energy required for crack growth is called critical energy release rate G_c. For pure modes, the critical condition for crack propagation is:

$$\begin{aligned} G_I &\geq G_{Ic} \\ G_{II} &\geq G_{IIc} \end{aligned} \tag{12}$$

However, when mode I and mode II are involved, the energy release rate is $G = G_I + G_{II}$. Then, the critical value of the energy release rate G_c when crack propagates depend on the mode ratio G_{II}/G. For instance, in a mixed mode test with a great mode ratio, G_c must be close to G_{IIc} and when the mode ratio is low G_c must be close to G_{Ic}. Thus, in spite of G_{Ic} and G_{IIc} being material properties, G_c is not.

In the previous study concerning the experimental assessment of ENFR [20], it was found that the linear criterion is suitable for representing the crack propagation in an ENFR test, where mode ratio varies during the test. Therefore, the condition for the crack propagation can be defined as:

$$\frac{G_I}{G_{Ic}} + \frac{G_{II}}{G_{IIc}} \geq 1 \tag{13}$$

Expressing Eq.(13) in similar form to Eq.(12), the crack propagation condition leads to:

$$G_I G_{IIc} + G_{II} G_{Ic} \geq G_{Ic} G_{IIc} \tag{14}$$

The left member of Eq. (12) is the energy available for a crack extension and the right member is the critical value for crack advance. Comparing Eq.(12) and Eq.(14) an equivalent energy release rate G_{eq} and an equivalent critical value G_{eqc} are defined as:

$$\begin{aligned} G_{eq} &= \left(G_I G_{IIc} + G_{II} G_{Ic} \right)^{1/2} \\ G_{eqc} &= \left(G_{Ic} G_{IIc} \right)^{1/2} \end{aligned} \tag{15}$$

Therefore, it can be stated then that crack propagates when:

$$G_{eq} \geq G_{eqc} \tag{16}$$

To the best knowledge of the authors, equivalent values of energy release rate given in Eq. (15) have not been previously defined.

4 ANALYSIS OF CRACK STABILITY

4.1 Stability definition

A general definition for stability is that a system is stable if a finite change in the input parameters does not cause an infinite change in the output values [27]. Regarding fracture tests carried out in universal testing machines, the input parameters are the load or the displacement applied by the testing machine and the output value is the crack length. Therefore, a fracture test is stable during crack growth when an infinitesimal change of the load or the displacement does not cause an infinite change in the crack length. According to Schwalbe et al [28], a crack extension under displacement control is stable when the crack stops when the applied displacement is held constant. In the present study, the stability condition is applied to the equivalent energy release rate G_{eq}:

$$\frac{dG_{eq}}{da} \leq \frac{dG_{eqc}}{da} \qquad and \qquad G_{eq} = G_{eqc} \tag{17}$$

Assuming that G_{eqc} is constant during crack growth, the stability criterion from Eq.(17) simplifies to:

$$\frac{dG_{eq}}{da} \leq 0 \tag{18}$$

Replacing Eq. (15) in the condition given in Eq.(18), the condition for stability can be expressed as follows:

$$\frac{dG_{eq}}{da} = \frac{1}{2}\left(G_I G_{IIc} + G_{II} G_{Ic}\right)^{-1/2}\left(\frac{dG_I}{da} G_{IIc} + \frac{dG_{II}}{da} G_{Ic}\right) \leq 0 \tag{19}$$

If the result of Eq.(19) is positive, then the crack growth is unstable, because the energy released is more than that needed to create a new surface area. If it is negative external work must be done to keep the crack moving.

It is worth noting that the equivalent energy release rate proposed is based on the fulfillment of the linear criterion. If that criterion is not suitable the present stability analisis is not valid.

4.2 Fixed load condition

Considering that $G_I = G_I(a,P)$and $G_{II} = G_{II}(a,P)$, the total derivative of the ERR due to each mode fracture with respect to the crack length, can be expressed as follows:

$$\frac{dG_I}{da}=\frac{\partial G_I}{\partial a}+\frac{\partial G_I}{\partial P}\frac{\partial P}{\partial a}$$
$$\frac{dG_{II}}{da}=\frac{\partial G_{II}}{\partial a}+\frac{\partial G_{II}}{\partial P}\frac{\partial P}{\partial a} \quad (20)$$

After applying the condition of constant load and replacing the values of G_I and G_{II} given in Eq. (10) in Eq. (20) it results:

$$\left(\frac{dG_I}{da}\right)_{Pcte}=\frac{\partial G_I}{\partial a}=-\frac{3E_f h^3 R^2}{(a-c)^5}-\frac{3PRc}{2b(a-c)^3}$$
$$\left(\frac{dG_{II}}{da}\right)_{Pcte}=\frac{\partial G_{II}}{\partial a}=\frac{9P^2 a}{8E_f b^2 h^3} \quad (21)$$

The stability condition of Eq.(19) leads to:

$$\left(\frac{dG_{eq}}{da}\right)_{Pcte}=\frac{1}{2}\left(\begin{array}{l}\left(\frac{3R^2E_fh^3}{4(a-c)^4}+\frac{3PRc}{4b(a-c)^2}+\frac{3P^2c^2}{16E_fb^2h^3}\right)G_{IIc}\\+\frac{9P^2a^2}{16E_fb^2h^3}G_{Ic}\end{array}\right)^{-1/2}\left(\left(-\frac{3E_fh^3R^2}{(a-c)^5}-\frac{3PRc}{2b(a-c)^3}\right)G_{IIc}+\frac{9P^2a}{8E_fb^2h^3}G_{Ic}\right)\leq 0 \quad (22)$$

Table 1 shows the properties of the carbon/epoxy unidirectional composite F593/T 300 used in the present study. These properties are obtained from a previous experimental assesment of the ENFR test [20] and the value of G_{eqc} is determined substituting the experimental values of G_{IC} and G_{IIC} in Eq. (15) The geometric dimensions used are span 2L=120mm, width b=15mm and thickness 2h=3mm.

Table 1 Mechanical properties of F593/T 300

Property	
E_{1f1} (MPa)	107,4
E_{22} (MPa)	10,6
G_{12} (MPa)	4,3
G_{Ic} (J/m^2)	263
G_{IIc} (J/m^2)	1152
G_{eqc} (J/m^2)	550

In order to determine the value of P that corresponds to each crack length of Eq.(22), a goal seeking process have been applied by means of the linear criterion, using the expressions of G_I and G_{II} of Eq.(10) and it can be expressed as follows:

$$\frac{G_I}{G_{Ic}} + \frac{G_{II}}{G_{IIc}} = 1 \tag{23}$$

For a given material and a given specimen geometry, the roller radius and the roller position can be varied to achieve a wide range of mode ratios G_{II}/G.

As it can be seen in Eq.(2), it is not possible to obtain an explicit expression of the normalized crack length a/L, due to the presence of the parameter c. Then, Fig. 3 shows the results of the derivative of G_{eq} of Eq.(22) that correspond to different crack lengths.

The nomenclature used in the legends of the figures is Ri-cj. Ri is the radius of the roller, and cj is the value of the c distance to the support where the roller is positioned. For instance, R0.5-c10 is the test where a roller with a radius of 0.5mm is positioned at 10 mm at the inner side of the support.

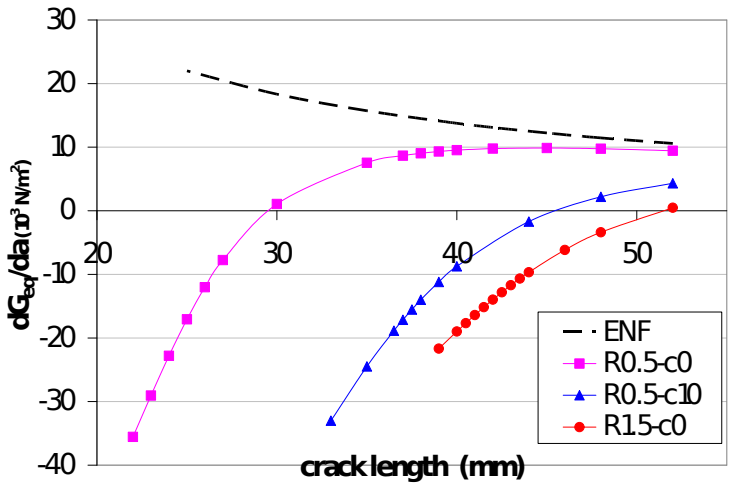

Fig. 3 Theoretical curves relating the derivative of G_{eq} to the crack length under load control.

As it can be seen in Fig. 3, for the same position of the roller, e.g. c=0, when the radius increases, the derivative of G_{eq} is negative in a wide range of crack lengths. For the same radius of the roller R=0.5mm, the instability starts in a longer crack length when it is positioned nearer to the crack tip. Therefore when R or c increase, the crack length range where the test is stable increases.

In the case of the pure mode II that corresponds to the ENF test it is always unstable. This agrees with the stability condition of the ENF test [14]. Moreover, all the tests have a common trend of going to a convergent positive value of the derivative of G_{eq}, therefore they seem prone to instability. Fig. 4 shows the stability condition in terms of the mode ratio.

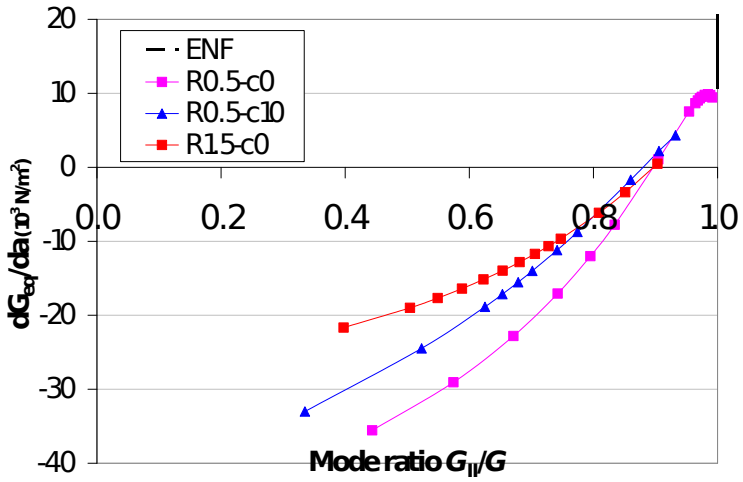

Fig. 4 Theoretical curves relating the derivative of G_{eq} to the mode ratio under load control dG_{eq}/da under load control versus mode ratio

When the mode ratio G_{II}/G increases, the test becomes more unstable. In fact, from mode ratio of 0.85 the derivative is positive and thus the test can be considered unstable.

4.3 Fixed displacement condition

Mechanical tests carried out in universal testing machines are considered to be at displacement control [26]. In order to determine the partial derivatives $\frac{\partial P}{\partial a}$ in Eq. (20) it is necessary to express the load as a function of the displacement and the crack lenght, i.e. $P=(a,\delta)$. From Eq.(2), the load can be expressed as follows:

$$P=\left(\delta+\frac{R}{4}\frac{(2a+c)}{(a-c)}\right)\left(\frac{8E_f bh^3}{3a^3+2L^3+c^3+3ac^2}\right) \tag{24}$$

Replacing the values of G_I and G_{II} given in Eq. (10) and the load given in Eq. (24) in Eq. (20), it results:

$$\begin{aligned}\left(\frac{dG_I}{da}\right)_{\delta cte}&=\left(-\frac{3E_f h^3R^2}{(a-c)^5}-\frac{3PRc}{2b(a-c)^3}\right)-\frac{9\left(P(a-c)^2c+2RE_f bh^3\right)^2}{8Eb^2h^3(a-c)^4(3a+c)}\\ \left(\frac{dG_{II}}{da}\right)_{\delta cte}&=\left(\frac{9P^2a}{8E_f b^2h^3}\right)-\frac{9Pa^2}{8E_f b^2h^3}\left(\frac{9Pa^2}{3a^3+2L^3}\right)=\frac{9P^2a}{4E_f b^2h^3}\left(\frac{-3a^3+L^3}{3a^3+2L^3}\right)\end{aligned} \tag{25}$$

The first terms of the second members Eq.(25) correspond to the derivatives of G_I and G_{II} under load control, as it can be seen in Eq.(21). The other terms are negative which means that crack propagation under displacement control is more stable. It is worth noting that, according to Eq.(25), the derivative of G_{II} with respect to the crack length agrees with the stability condition for the ENF test [14]. Replacing

results of Eq.(25) into Eq.(19) the stability condition under displacement control can be expressed as follows:

$$\left(\frac{dG_{eq}}{da}\right)_{\delta cte} = \frac{1}{2}\left(\left(\left(\frac{dG_I}{da}\right)_{Pcte} - \frac{9\left(P(a-c)^2c + 2RE_f bh^3\right)^2}{8E_f b^2h^3(a-c)^4(3a+c)}\right)G_{IIc} + \left(\left(\frac{dG_{II}}{da}\right)_{Pcte} - \frac{9Pa^2}{8E_f b^2h^3}\left(\frac{9Pa^2}{3a^3+2L^3}\right)\right)G_{Ic}\right)^{-1/2} \quad \left(G_I G_{IIc} + G_{II} G_{Ic}\right) \le 0 \qquad (26)$$

Fig. 5 shows Eq. (26) applied to different test conditions.

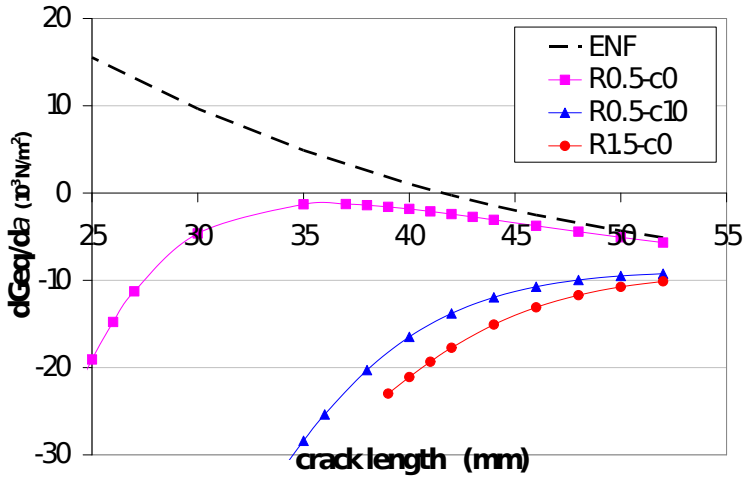

Fig. 5 Theoretical curves relating the derivative of G_{eq} to the crack length under load control

Except for the ENF test, all the test conditions that have been studied are stable. In the ENF test, the stability limit is a=42 mm which corresponds to the stability value of a/L=0.7 [14]. Moreover, all the tests have a common trend of going to a convergent negative value of the derivative of G_{eq}. In the case of R0.5-c0, the curve has a maximum value near zero when the crack length is about 35mm. It can be concluded that for a lower radius the curve of the derivative could be positive.

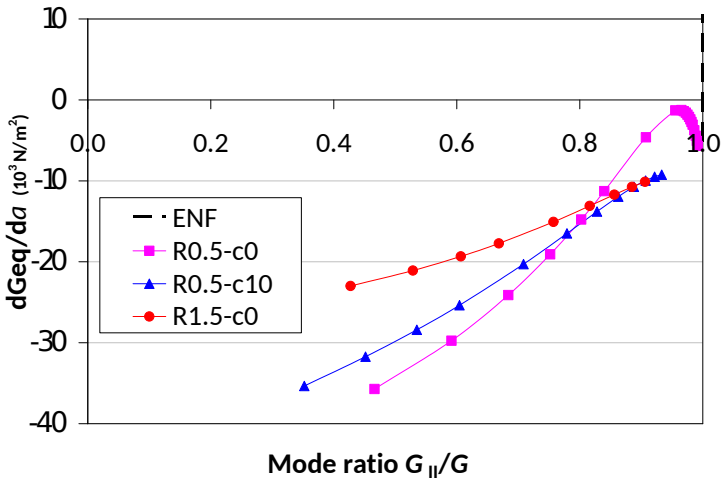

Fig. 6 Theoretical curves relating the derivative of G_{eq} to the mode ratio under displacement control dG_{eq}/da under displacement control versus mode ratio

Fig. 6 shows the derivative of G_{eq} versus mode ratio G_{II}/G. Low values of the mode ratio, which are related with a shorter crack length for fixed vaues of c, R, give greater negative values of the derivative.

Therefore under displacement control, for radii between 0.5mm and 1.5mm, and roller position between c=0 and c=10, which cover a wide range of mixed mode ratios from 0.35 up to 0.98, all the test conditions can be considered as stable.

5 ERROR ANALYSIS

The error in the determination of G_{eq} depends on the determination of the crack length and that depends on the experimental value of the compliance. Consequently, a two step error analysis is performed: in the first step, it is analyzed how a possible error in the measurement of the experimental compliance affects the determination of the crack length. In the second step it is analyzed how a possible error in the crack length affects the determination of G_{eq}. For that purpose, partial derivative of the compliance of the test of Eq.(4) with respect to a and the partial derivative of the G_{eq} of Eq. with respect to a, have been determined, resulting in:

$$\frac{\partial C}{\partial a} = \frac{9a^2 + 3c^2}{8E_f bh^3}$$
$$\frac{\partial G_{eq}}{\partial a} = \frac{1}{2}\left(G_I G_{IIc} + G_{II} G_{Ic}\right)^{-1/2}\left(\left(-\frac{3E_f h^3 R^2}{(a-c)^5} - \frac{3PRc}{2b(a-c)^3}\right)G_{IIc} + \frac{9P^2 a}{8E_f b^2 h^3} G_{Ic}\right) \quad (27)$$

If the variation of a is small, the derivatives can be assumed as increments. Taking into account that the crack determination is based on the variation of the experimental compliance, the relative errors are:

$$\frac{\Delta a}{a} = K_{Ca}\left[\frac{\Delta C}{C}\right]_a \qquad K_{Ca} = \frac{8E_f bh^3}{9a^2+3c^2}\frac{C}{a} = \frac{3a^3+2L^3+c^3+3ac^2}{9a^3+3ac^2}$$

$$\left[\frac{\Delta G_{eq}}{G_{eq}}\right]_a = K_{aG}\frac{\Delta a}{a} \qquad K_{aG} = \frac{a}{2}\left(G_I G_{IIc} + G_{II} G_{Ic}\right)^{-1}\left(\left(-\frac{3E_f h^3 R^2}{(a-c)^5} - \frac{3PRc}{2b(a-c)^3}\right)G_{IIc} + \frac{9P^2 a}{8E_f b^2 h^3}G_{Ic}\right) \tag{28}$$

The absolute value of K_{Ca} coefficient of Eq. gives the output relative error in a, with respect to the relative input error of C. For instance, if the absolute value of K_{Ca} is equal to 1, the relative error in the determination of a has the same value as the relative error of the measurement of C.

The absolute value of K_{aG} coefficient of Eq. gives the relative output error in G_{eq}, with respect to the relative input error of a. In order to analyze the influence of these coefficients, the material properties of **Table 1** and the same test conditions and geometric dimensions as those studied in section 4 are utilized. The results are depicted in Fig. 7 and Fig. 8.

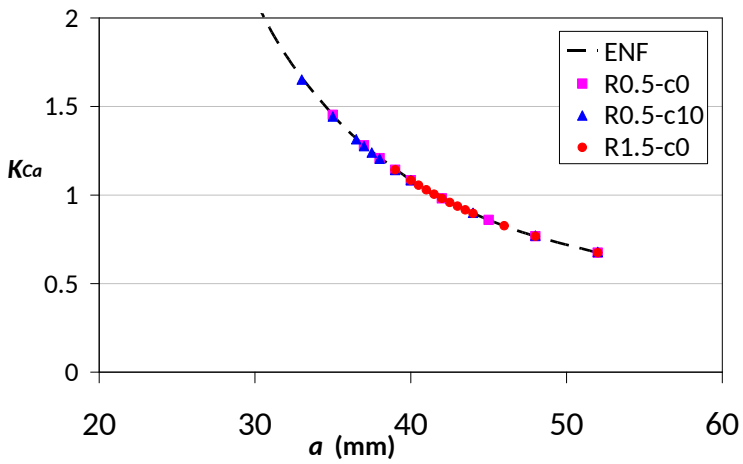

Fig. 7 Influence of the compliance relative error on the relative error of crack length.

According to Fig. 7, K_{Ca} takes always the same value regardless of the test conditions. Its value is less than 1 for initial crack length values greater than 42mm. This means the relative error in the determination of a is lower than the error committed in the measurement of the experimental compliance. As it is shown in Fig. 7, when the crack length is very short, less than 35mm the value of K_{Ca} grows sharply. Consequently, it is recommended to use crack lengths greater than 35mm.

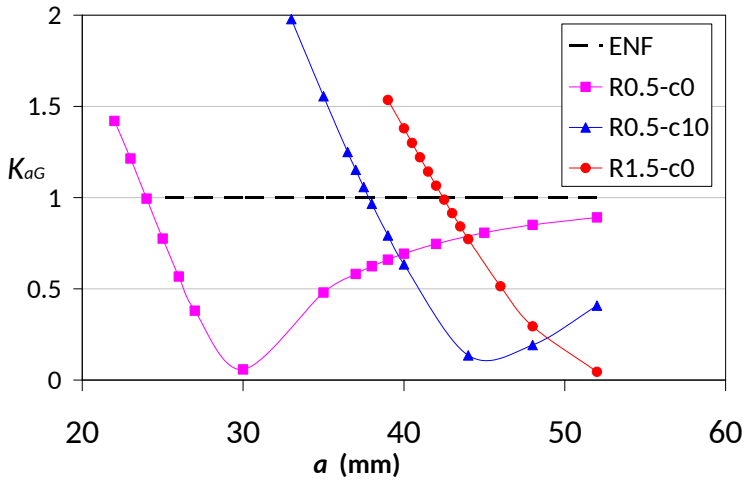

Fig. 8 Influence of crack length relative error on the relative error of G_{eq}

Fig. 8 shows the absolute value of the coefficient K_{aG} for different test conditions. In the ENF test, K_{aG} =1 for any crack length since in Eq.(28) G_I=0. In the case of R0.5-c0, when the crack length a>24mm the absolute value of K_{aG} is below 1. Moreover, there is a minimum value when a=30mm. In the case of R0.5-c10, the curve has a similar shape but the crack length should be a>39mm to get a value of K_{aG} below 1, and the minimum value corresponds to a=45mm. In the case of R1.5-c10 when a>43mm it gives an absolute value of K_{aG} below 1, being the minimum value when a=52mm. Therefore when R or c increase, the minimum crack length to get K_{aG}<1 increases.

According to Eq.(28), it is possible to analyze directly the influence of the relative input error of the compliance in the relative output error of G_{eq} as it follows

$$\left[\frac{\Delta G_{eq}}{G_{eq}}\right]_a = K_{aG}K_{Ca}\left[\frac{\Delta C}{C}\right]_a \tag{29}$$

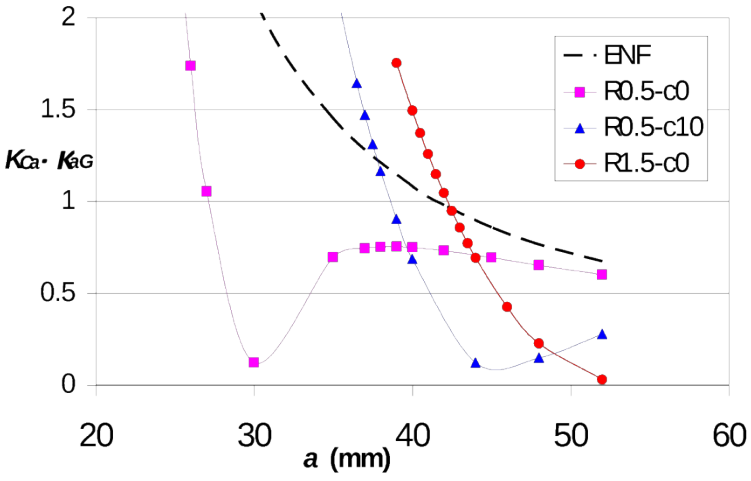

Fig. 9 Influence of compliance relative error on the relative error of G_{eq}

Fig. 9 shows the absolute value of the product of two coefficients K_{aG} $K_{Ca.}$ The absolute values of the product K_{aG} $K_{Ca.}$ lower than 1 take place in similar crack lengths to those obtained in the analysis of K_{aG}. In order to determine an optimum test condition, the product of K_{aG} K_{Ca} should be taken into account.

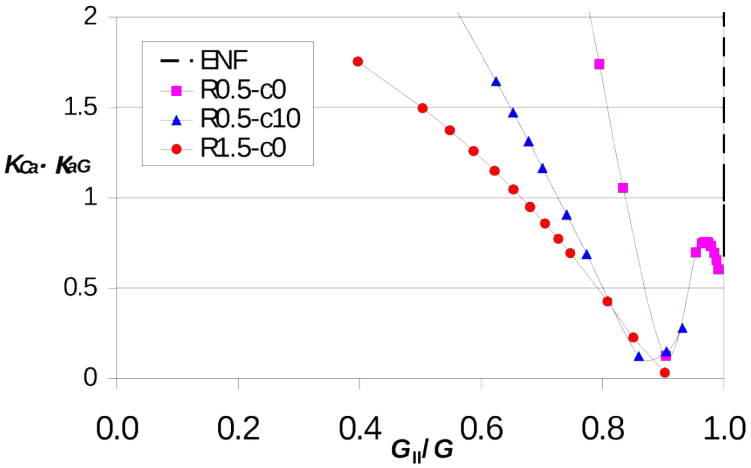

Fig. 10 Absolute value of K_{aG} K_{Ca} versus mode ratio G_{II}/G

Fig. 10 shows the absolute value of K_{aG} K_{Ca} versus mode ratio G_{II}/G. When the mode ratio is greater, which is related to a longer crack length for fixed vaues of c, R, the absolute value of K_{aG} K_{Ca} is lower. Thus it means that the relative error of G_{eq} is reduced with respect to the relative error of the experimental compliance.

Table 2 summarizes the optimum crack lengths depending on the different criteria.

Table 2 Optimum crack lengths in mm.

	STABILITY CONDITION		ERROR ANALYSIS		
TEST NOMENCLATURE	Load Control	Displacement control	K_{Ca}<1	K_{aG}<1	K_{aG} K_{Ca}<1
ENF	Not stable	a > 42	a > 42	K_{aG}=1	a > 42
R0.5-c0	a < 30	stable	a > 42	a > 24	a > 27
R0.5-c10	a < 45	stable	a > 42	a > 38	a > 39
R1.5-c0	a < 51	stable	a > 42	a > 43	a > 43

In order to define optimum test conditions, the crack length has to satisfy the stability condition and to minimize the relative error in the determination of G_{eq}.

6 EXPERIMENTAL

6.1 Materials and test apparatus

T6T/F593 prepregs provided by Hexcel Composites with a 55% volume-content of fibre were used to produce laminates. The plates were manufactured by hot press molding. Sixteen-layered unidirectional laminates, $[0]_{16}$, were made with a Teflon film introduced centered during the piling up process in order to make the initial crack. The specimens were cut with a diamond disc saw, being the nominal thickness and width 3 mm and 15 mm, respectively. The edges of the laminate were discarded for the preparation of the specimens. Tests were performed on an MTS-Insight 100 electromechanical testing machine equipped with a 5kN load cell, operating in a displacement controlled mode. In order to avoid the influence of the resin rich area the specimens were precracked in mode II by a ENF test, increasing the cracked length around 5 mm.

All the specimens were tested using a procedure based on three-point bending tests at five different spans proposed by Mujika [29], in order to obtain the flexural modulus, E_f and the out of plane shear modulus $G_{LT'}$, which is equal to the in-of-plane shear modulus G_{LT} assuming that the material is transversely isotropic. The mean values corresponding to five specimens were:

E_f = 107.4 (±1.4) GPa

$G_{LT'}$ = 4.3 (±0.4) GPa

6.2 Experimental test conditions

Several mixed mode tests have been performed in order to compare the results with the ones obtained applying the theoretical stability condition. The experimental displacement is defined as 0 when the contact between the load nose and the specimen without roller occurs, as it is shown in Fig. 11. After inserting the roller, there is an initial negative displacement δ_0 for the zero load condition, as seen in Fig. 2. Actually, the contact in the testing machine has been defined when the load was 0.5 N.

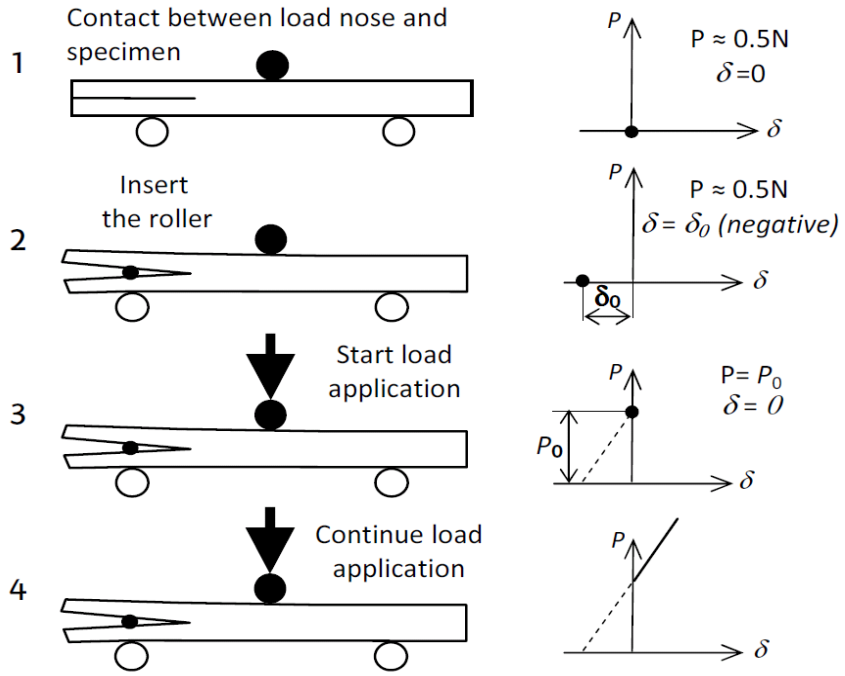

Fig. 11 Initial Conditions in Load-Displacement curve

The determination of the crack length at every point where P and δ are measured, is based on the variation of the compliance during the crack advance, based on the Beam Theory including Bending Rotation effects (BTBR) method developed for the ENF test by Arrese et al [30]. For the experimental analysis bending rotation effects have not been included because the support roller radii are 2.5mm and thus the influence is negligible [30]. In a previous work [20], it was verified that in the ENFR test the crack length can be determined without optical methods. In spite of only bending effects have been presented for simplicity in the analytical background, the calculations concerning the experimental part have been carried out including also shear effects.

Since the contribution of each fracture mode varies during the crack propagation, the mode ratio at the initiation point is the parameter chosen to define the type of mixed mode test. To determine that initial mode ratio, the value of energy release rate for each mode contribution has been determined substituting the value of the crack length in Eq.(10), when Δa=0.25mm, considering it as nonlinearity point (NL). The NL point is one of the definitions of crack initiation presented in the standard [12].

The nomenclature that has been used in order to identify each test condition is ai-Rj-ck. ai is the nominal initial crack length; Rj is the inserted roller radius; and ck is the value of the c distance that defines the position of the roller. For instance, a40-R1-c8 is the test with initial nominal crack length of 40 mm, an inserted roller of 1mm radius and positioned at 8mm at the inner side of the support.

The nominal geometric dimensions are span 2*L*=120mm, width *b*=15mm and thickness 2*h*=3mm.

All the test conditions are summarized in Table 3. For simplicity, a number will be used in the legends of the graphics.

Table 3 Summary of experimental test conditions

ID	NOMENCLATURE	INITIAL GII/G (%)
Test 1	a40-R0.5-c0	96
Test 2	a31-R0.5-c0	90
Test 3	a45-R1.5-c0	74
Test 4	a43-R0.9-c8	66
Test 5	a38-R0.7-c8	59

6.3 Results and discussion

6.3.1 Energy release rate curves

The determination of the crack length at any point of the test where P and δ are measured, allows the calculation of the energy release rate at any point during the crack propagation. The experimental values of G_I and G_{II} of the tests presented in Table 3, have been obtained substituting the value of the crack length, in Eq.(10). In Fig. 12 the experimental energy release rate curves due to each mode can be seen. In the legend of the figures besides the identifier of the test the initial mode ratio is included in brackets.

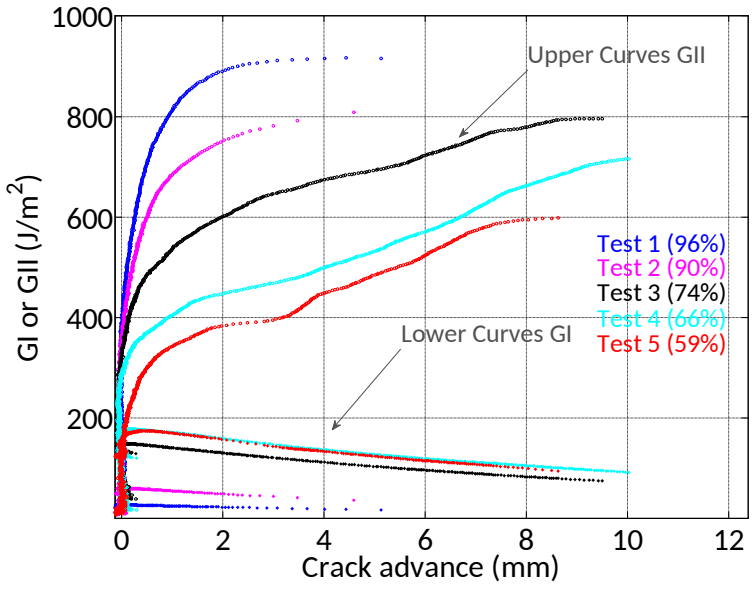

Fig. 12 Experimental Energy Release Curves

As it can be seen in Fig. 12, the upper curves correspond to G_{II}, and the lower ones to G_I. The curve of G_I and the curve of G_{II} that correspond to the same test condition are drawn with the same color. When crack propagates, the curves of G_I decrease slowly. At the same time, the curves for G_{II} increase. This means that the contribution of each mode is changing during crack propagation.

In Fig. 13 the total energy release rate $G = G_I + G_{II}$ is depicted.

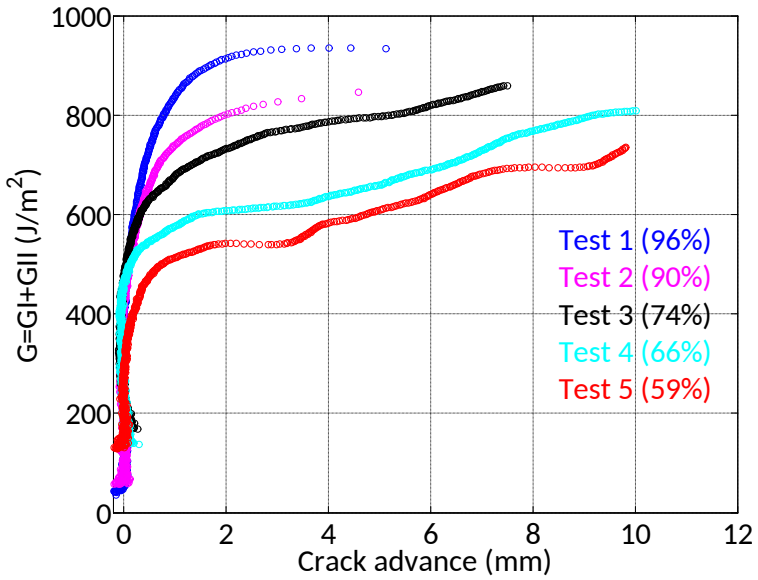

Fig. 13 Experimental total Energy Release Rate

When the mode II is predominant the total energy release rate tends to a constant value. When the mode I is more important the total G increases with crack advance. Those trends agree qualitatively with the results obtained in R-curves of the pure modes concerning ENF and DCB tests, respectively: a plateau in ENF tests [30] and the increase of G in DCB tests for the same material [31].

6.3.2 Linear criterion, normalized mode ratios and equivalent energy release rate curves

In the previous study concerning the experimental assessment of ENFR [20], it was found that the linear criterion of Eq.(23) is suitable for representing the crack propagation in an ENFR test, where mode ratio varies during the test.

The value of G_{IIc} is four times G_{Ic} in the case of the material used in this study as it can be seen in **Table 1**. Therefore, in order to analyze the direct contribution of each mode to failure, instead of G_I and G_{II}, normalized mode ratios have been defined [20]:

$$\frac{G_I}{G_{Ic}} = G_I^0 \qquad \frac{G_{II}}{G_{IIc}} = G_{II}^0 \tag{30}$$

These normalized mode ratios of Eq.(30) are the summands of the linear criterion. The initial values of the total and the normalized mode ratios given in Eq.(30) are shown in Table 4.

Table 4 Initial mode ratio and initial normalized mode ratio

ID	INITIAL MODE RATIO (G_{II}/G) (%)	INITIAL NORMALIZED MODE RATIO (G_{II}^0) (%)
Test 1	96	51
Test 2	90	45
Test 3	74	37
Test 4	66	30
Test 5	59	22

The test with the highest initial mode ratio and the one with the lowest mode ratio have been plotted in Fig. 14 in terms of the normalized mode ratios.

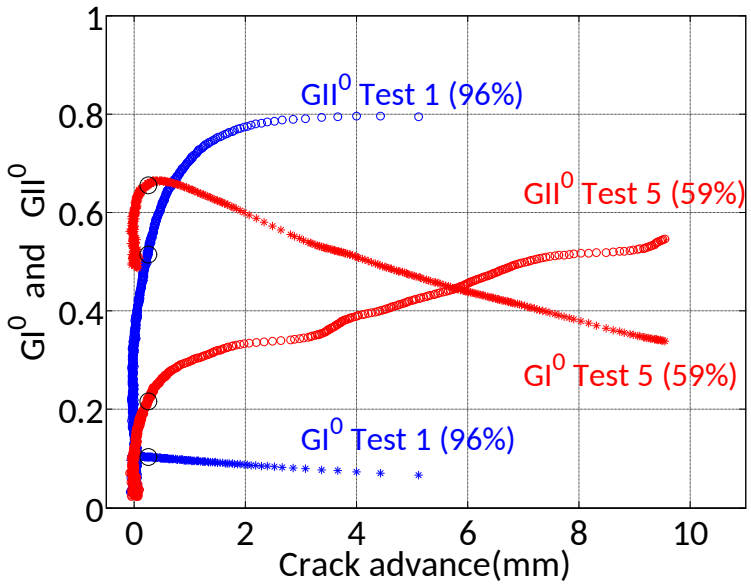

Fig. 14 Experimental normalized mode ratios $G_I^0$and G_{II}^0

When the mode II is clearly predominant the G_{II}^0 curve is above the G_I^0 curve, as in Fig. 12. Nevertheless, when the initial mode ratio is 59%, the curve of G_I^0 is above the curve of G_{II}^0 during almost all the propagation, in contrast to what happened with G_{II} and G_I.

As linear criterion is adopted, the sum of the two normalized mode ratios G_I^0+G_{II}^0 depicted in Fig. 15, should be close to 1.

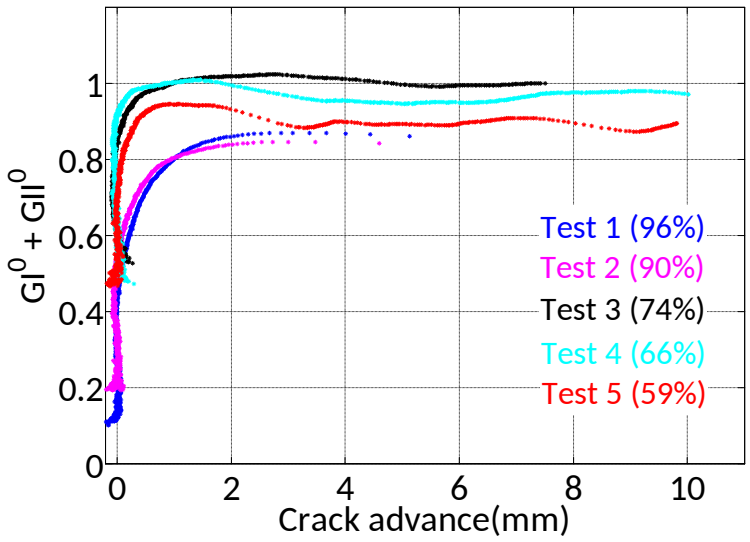

Fig. 15 Sum of experimental normalized mode ratios

The mean value of the curves during propagation is always higher than 0.85, and in the case of tests 3 and 4 is very close to 1. The maximum deviation occurs in the tests with mode ratio near to pure mode II, tests 1 and 2, and the maximum relative error is 15% with respect to the linear criterion.

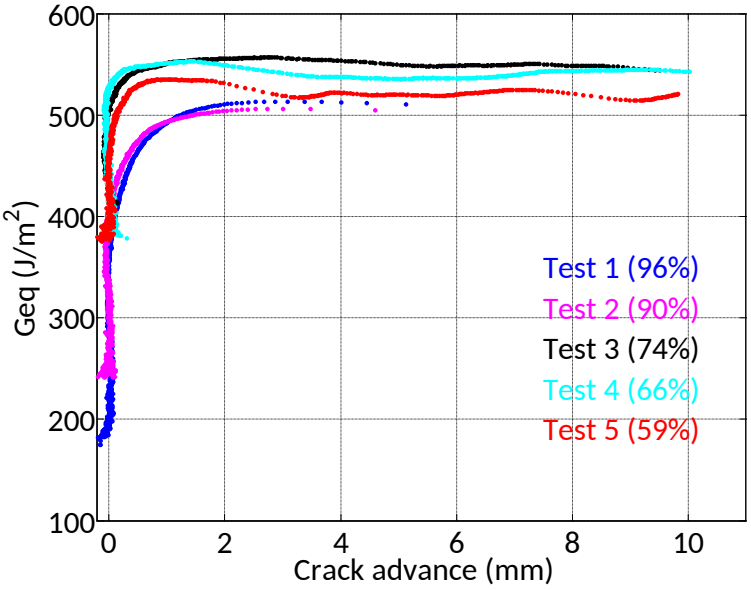

Fig. 16 Equivalent ERR, experimental G_{eq}

The proposed equivalent energy release rate of Eq. (15) has been applied to the experimental data and the results are presented in Fig. 16. In all the cases the equivalent ERR tends to a constant value. The mean values of the curves during propagation are between 505 and 555 (J/m^2). The value of the plateau agrees with the theoretical value of G_{Ceq}=550 (J/m^2) of **Table 1**. The maximum deviation corresponds to the tests 1 and 2 and in those cases the maximum relative error is 8.5% with respect to the theoretical

value of G_{Ceq}.Consequently, according to the results shown in Fig. 16, the proposed equivalent ERR approach can be considered suitable for defining crack propagation condition of the ENFR test.

6.3.3 Stability evaluation

During the testing phase, it has been assumed that unstable crack growth occurs when there is a jump in the load-displacement curve. In Fig. 17 the load-displacement curves of the tests presented in Table 3 are presented. The circular marker included in figures indicates the crack inititation point or the NL point.

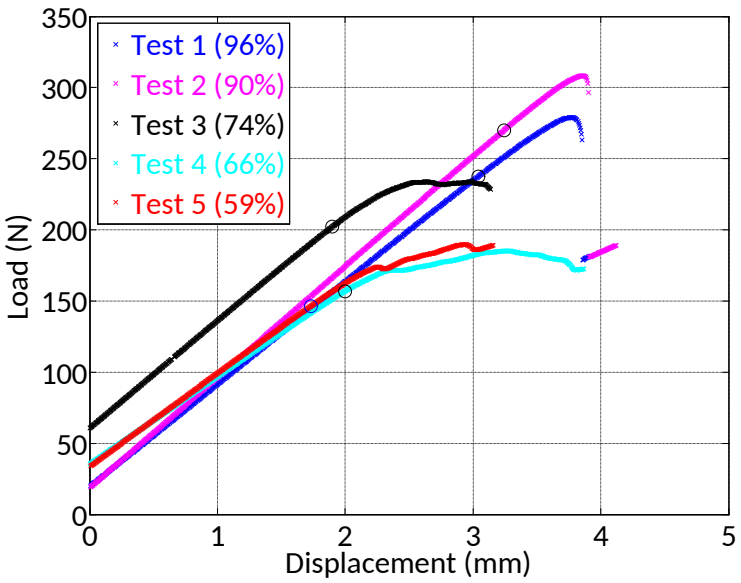

Fig. 17 Experimental load-displacement curves

When the initial mode ratio is close to pure mode II, tests 1 and 2, when the crack starts to propagate the load continues increasing, which means that it is behaving in a stable manner. After the load reaches its maximum value it decreases suddenly. Besides, there are jumps in both curves. Therefore the tests 1 and 2 can be considered stable during the most part of the propagation, and at the final stage they become unstable. In the rest of the cases, there are not jumps or sudden load drops during crack propagation. It can be concluded then, that they are all stable.

The definition of stability of section 4.1, which defines a test as stable if an infinitesimal change of displacement, does not cause an infinite change in the crack length, has been taken into account to analyze the experimental data. In Fig. 18 the relationship between crack length and the displacement is depicted.

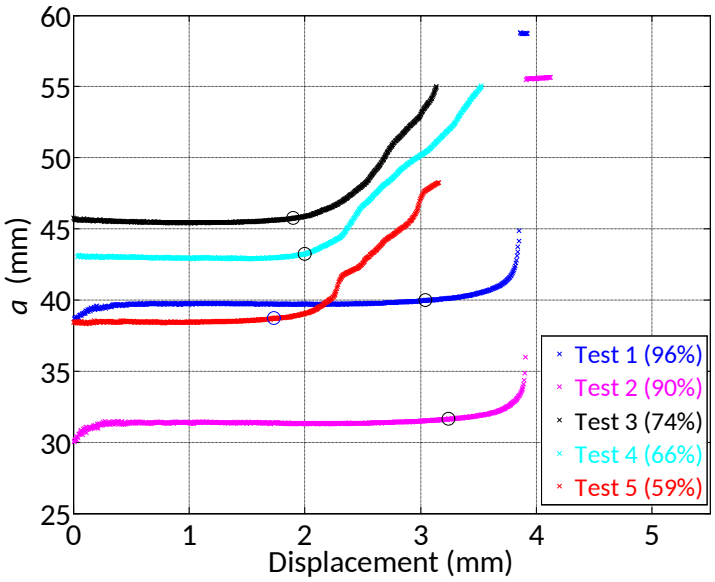

Fig. 18 Crack length versus displacement

In the curves of tests 1 and 2 at the first stage of the propagation, a finite change in displacement causes a finite change in the crack length and thus they can be considered stable. However, at the final stage of the propagation a small change in displacement causes a much greater change in crack length, and there are even jumps in the curve. Therefore, they become unstable.

For the rest of the tests, the crack propagation starts earlier, and the slope of the curve is similar, which means that a finite change in the displacement is needed to have a finite change in the crack length. Consequently, they are all stable according to this definition.

This is the same conclusion drawn by analyzing P-δ curves.

Since the experimental tests have been carried out at a constant displacement rate which means under displacement control, theoretical stability condition based on the derivative of $G_{eq,}$ of Eq. (26) is applied to the experimental data.

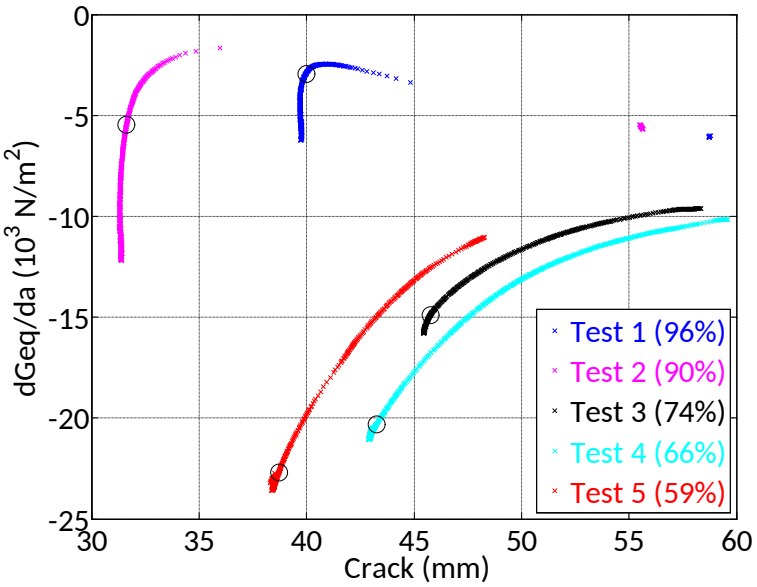

Fig. 19 Stability condition applied to experimental data

As it can be seen in Fig. 19 in the cases of tests 1 and 2, the values of the derivative during propagation are quite close to the zero value which is the limit of the stability. Nevertheless, all the tests fulfill the stability condition since the value of the derivative is always negative. In the tests with lower initial mode ratio, the value of the derivative is even smaller than those of tests 1 and 2, and therefore they are supposed to be more stable. In Fig. 20 the stability condition of Eq. (26) in terms of mode ratio can be seen.

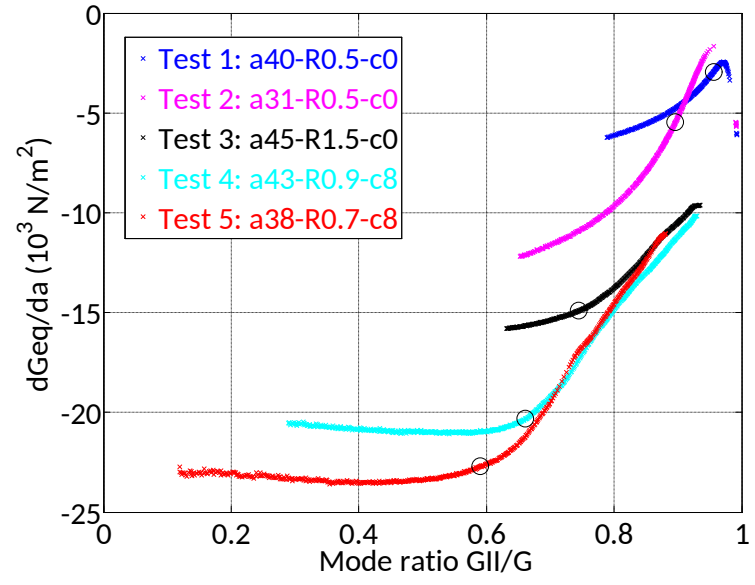

Fig. 20 Stability condition versus mode ratio

When the crack grows the mode ratio increases and although the derivative remains negative, it is close to positive values. This agrees with the theoretical analysis of stability under displacement control depicted in Fig. 6.

As a general conclusion, the stability condition for the ENFR test proposed in Eq.(26) agrees reasonably with the experimental stability based on different definitions.

6.3.4 Test recommendations

Concerning tests performed under displacement control, proper values for the initial crack length, the radius and the position of the roller are suggested according to the theoretical stability condition shown in Fig. 5 and its experimental assessment shown in Fig. 19: For radii of the roller between $0.5 < R < 1.5$mm, since greater radius lead to geometric non-linearities, and roller positions between values of $0 < c < 10$mm, all the tests are stable for crack lengths between $35 < a < 52$mm.

Therefore, within those values, the optimum test conditions are the ones that satisfy the linear failure criterion. According to the quality of linear criterion shown in Fig. 15 and according to G_{eq} depicted in Fig. 16 the optimum test conditions are the ones with an initial mode ratio in the range 65-75% in agreement with previous results [20].

Taking into account the influence of the experimental compliance measurement on the crack length and on the equivalent ERR shown in Table 2, the optimum crack length depends on R and c, but in general should be greater than 42mm for the material and specimen dimensions used in the present study.

7 SUMMARY AND CONCLUSIONS

Based on the reliability of the linear criterion, an equivalent energy release rate G_{eq} has been proposed taking into account the interaction between the two modes included in the ENFR mixed-mode test. Experimental results obtained with specimens of F593/T300 carbon/epoxy unidirectional composite show a good agreement with the proposed approach. Furthermore, during crack propagation the critical value of G_{eq}, namely G_{eqc}, reaches a plateau value similar for different test conditions that can be considered a material property.

An error analysis has been performed in order to study the influence of the experimental compliance measurement on the crack length and on the G_{eq}. Moreover, the influence of the crack length on the G_{eq} has been analized.

The stability of the crack propagation of the ENFR mixed mode test has been defined by means of the derivative of G_{eq}. The experimental results have been assessed analyzing the crack growth behaviour under the applied displacement. It has been concluded that all the tests studied, carried out under displacement control, show stable crack propagation.

Some test recommendations have been suggested in order to define a stable test under displacement control. The test conditions with an initial mode ratio in the range 65-75% can be considered the most suitable ones according to the quality of fulfillment of the linear criterion.

8 REFERENCES

[1] AB Pereira, AB de Morais. Mixed mode I + II interlaminar fracture of carbon/epoxy laminates, Composites Part A: Applied Science and Manufacturing. 39 (2008) 322-333.

[2] European Structural Integrity Society (ESIS), Determination of the mixed-mode I/II delamination resistance of unidirectional fibre-reinforced polymer laminates using the asymmetric double cantilever beam specimen (ADCB), (2000).

[3] BRK Blackman, AJ Brunner, P Davies. Delamination fracture of continuous fibre composites: Mixed-mode fracture, European Structural Integrity Society. 28 (2001) 335-359.

[4] JMQ Oliveira, MFSF de Moura, JJL Morais. Application of the end loaded split and single-leg bending tests to the mixed-mode fracture characterization of wood, Holzforschung. 63 (2009) 597-602.

[5] H Yoshihara. Initiation and propagation fracture toughness of solid wood under the mixed Mode I/II condition examined by mixed-mode bending test, Eng.Fract.Mech. 104 (2013) 1-15.

[6] PN Anh, M Stéphane, C Myriam, C Jean-Luc. R-curve on Fracture Criteria for Mixed-mode in Crack Propagation in Quasi-brittle Material: Application for Wood, Procedia Materials Science. 3 (2014) 973-978.

[7] FJP Chaves, LFM da Silva, MFSF de Moura, DA Dillard, VHC Esteves. Fracture Mechanics Tests in Adhesively Bonded Joints: A Literature Review, J.Adhesion. 90 (2014) 955-992.

[8] BRK Blackman, AJ Kinloch, FS Rodriguez-Sanchez, WS Teo. The fracture behaviour of adhesively-bonded composite joints: Effects of rate of test and mode of loading, Int.J.Solids Structures. 49 (2012) 1434-1452.

[9] N Ben Salem, J Jumel, MK Budzik, MER Shanahan, F Lavelle. Analytical and experimental investigations of crack propagation in adhesively bonded joints with the Mixed Mode Bending (MMB) test Part I: Macroscopic analysis & Digital Image Correlation measurements, Theor.Appl.Fract.Mech. 74 (2014) 209-221.

[10] N Ben Salem, J Jumel, MK Budzik, MER Shanahan, F Lavelle. Analytical and experimental investigations of crack propagation in adhesively bonded joints with the Mixed Mode Bending (MMB) test Part II: Investigation of cohesive stresses distribution with backface strain monitoring, Theor.Appl.Fract.Mech. 74 (2014) 222-232.

[11] J Mohan, A Ivanković, N Murphy. Mixed-mode fracture toughness of co-cured and secondary bonded composite joints, Eng.Fract.Mech. 134 (2015) 148-167.

[12] ASTM D6671-01. Standard test method for mixed mode I-mode II interlaminar fracture toughness of unidirectional fiber-reinforced polymer matrix composites (2006).

[13] R Olsson. A simplified improved beam analysis of the DCB specimen, Composites Sci.Technol. 43 (1992) 329-338.

[14] LA Carlsson, JW Gillespie JR, RB Pipes. On the Analysis and Design of the End Notched Flexure (ENF) Specimen for Mode II Testing, Journal of Composite Materials. 20 (1986) 594-604.

[15] H CHAI, S MALL. Design Aspects of the End-Notch Adhesive Joint Specimen, Int.J.Fract. 36 (1988) R3-R8.

[16] D Phillips, G Wells. The Stability of Transverse Cracks in Fiber Composites, J.Mater.Sci.Lett. 1 (1982) 321-324.

[17] O Allix, A Corigliano. Modeling and simulation of crack propagation in mixed-modes interlaminar fracture specimens, Int.J.Fract. 77 (1996) 111-140.

[18] A Szekrenyes. Crack Stability of Fracture Specimens used to Test Unidirectional Fiber Reinforced Material, Exp.Mech. 50 (2010) 473-482.

[19] A Boyano, V Mollón, J Bonhomme, J De Gracia, A Arrese, F Mujika. Analytical and numerical approach of an End Notched Flexure test configuration with an inserted roller for promoting mixed mode I/II, Eng.Fract.Mech. 143 (2015) 63-79.

[20] A Boyano, J De Gracia, A Arrese, F Mujika. Experimental assessment of an End Notched Flexure test configuration with an inserted roller for analyzing mixed-mode I/II fracture toughness, Eng.Fract.Mech. 163 (2016) 462-475.

[21] AA Griffith. The Phenomena of Rupture and Flow in Solids, Philosophical Transactions of the Royal Society of London.Series A, Containing Papers of a Mathematical or Physical Character. 221 (1921) 163-198.

[22] GR Irwin. Onset of Fast Crack Propagation in High Strength Steel and Aluminium Alloys, SagamoreResearch Conference Proceedings. 2 (1956) 289-305.

[23] JG Williams. On the calculation of energy release rates for cracked laminates, Int.J.Fract. 36 (1988) 101-119.

[24] A Szekrenyes. Prestressed fracture specimen for delamination testing of composites, Int.J.Fract. 139 (2006) 213-237.

[25] MF Kanninen, CL Popelar, Advanced fracture mechanics, OXFORD UNIVERSITY PRESS, New York, 1985.

[26] TL Anderson, Fracture mechanics :fundamentals and applications, 3rd ed., CRC Press 2005.

[27] Z Bazant, L Cedolin. Stability of structures: elastic, inelastic, fracture, and damage theoriesOxford University Press, Inc, New York. (1991).

[28] K Schwalbe, I Scheider, A Cornec, Guidelines for applying cohesive models to the damage behaviour of engineering materials and structures, Springer Science & Business Media 2012.

[29] F Mujika. On the effect of shear and local deformation in three-point bending tests, Polym.Test. 26 (2007) 869-877.

[30] A Arrese, N Carbajal, G Vargas, F Mujika. A new method for determining mode II R-curve by the End-Notched Flexure test, Eng.Fract.Mech. 77 (2010) 51-70.

[31] J De Gracia, A Boyano, A Arrese, F Mujika. A new approach for determining the R-curve in DCB tests without optical measurements, Eng.Fract.Mech. 135 (2015) 274-285.